JOURNAL OF MATERIALS SCIENCE **37** (2002) 3973–3979

Characterisation of porous ceramic plugs for use in electrochemical sensors

R. W. BOSCH, S. STRAETMANS, S. VAN DYCK
SCK•CEN, Nuclear Research Centre Belgium, Boeretang 200, B-2400 Mol, Belgium
E-mail: rbosch@sckcen.be

In electrochemical sensors like pH-, reference- or ion-selective electrodes a porous ceramic plug (or diaphragm) maintains the conducting junction with the test solution. These liquid junctions should have a resistance as low as possible meanwhile avoiding leakage through the junction. Five porous magnesium stabilised zirconium oxide plugs with different porosity's and pore size (distribution) were investigated as liquid junctions. The physical properties of these porous plugs were investigated with SEM and Mercury Intrusion Porosimetry. Important working conditions of these porous plugs are the resistance of the porous plug filled with an electrolyte and the contamination speed through these porous plugs, both for the test solution as the reference solution. The first property was measured by a 4-wire resistance measurement. The second property was measured by measuring the flow through rate of the reference electrolyte through the plug. It was shown that an optimal plug i.e., low leakage and high conductivity through the membrane, had a high porosity and relative small pores (0.25 μm). A simple mathematical model based on the Hagen-Poiseuille equation was developed to describe the porous plug characteristics. It was shown that mathematical calculation of the porous plug resistance was in good agreement with experimental results.

1. Introduction

Most electrochemical sensors, like pH-electrodes, reference electrodes and Ion Selective Electrodes (ISE) use a porous ceramic plug to maintain a conducting connection between the reference electrode and the test solution [1–3]. Specially in the design of high temperature reference electrodes to be used for electrochemical measurements in aqueous solution at elevated temperatures, this porous plug is an important part of the design [4–9]. The porous plug should minimise the contamination of the test solution by the reference solution (for example to avoid chloride contamination of the test solution) and vice versa. The potential of the reference electrode depends on the reference solution, so contamination (or dilution) of the reference solution will result in drift of the reference electrode potential. On the other hand the liquid junction connection should be as conductive ad possible to minimise the reference electrode impedance. To optimise the design of such a porous plug, five porous plugs of magnesium stabilised zirconium oxide were produced with different pore size and porosity. Different measurement techniques were employed to characterise the porous plugs. SEM and Mercury Intrusion Porosimetry were used to obtain the physical properties of the porous plugs. Solution resistance measurements through the plug and the flow through rate of the electrolyte solution of the reference electrode (typical a 0.1 M KCl solution) were used to characterise the working conditions of the plug. The resistances and flow through rates were compared with the physical properties to find the optimum porous plug design.

Also a simple mathematical model based on the Hagen-Poiseuille equation was developed to describe the porous plug characteristics. With this model and the results of the flow-through measurements, the resistance of a porous plug soaked with electrolyte solution could be determined.

2. Production of the porous zirconia plugs

The magnesium stabilised zirconium powder was obtained from a commercial company. The composition of the powder is given in Table I. The magnesium oxide is a stabilising oxide which forms a solid solution with the zirconia and give rise to a structure which is a mixture of cubic and monoclinic zirconia. The magnesium stabilised zirconium oxide powder of certain size (typically particle size smaller than 10 μm) was pressed to small cylinders by CIP (Cold Isostatic Pressure). Then these cylinders were sintered at various times and temperature to produce porous plugs with different porosity and pore size. Table II shows the sinter temperatures of the different porous plugs.

Typical size of a porous plug is a diameter of 3.5 mm and a length of 10 mm. Fig. 1 shows a photograph of some of these porous zirconia plugs.

TABLE I Composition of the magnesium stabilized zirconium powder

Material	Weight percentage
$ZrO_2 + HfO_2$	96.00
MgO	3.50
TiO_2	0.15
SiO_2	0.12
Al_2O_3	0.08
Fe_2O_3	0.06
Na_2O	<0.10
Alkaline earth metal oxides	<0.20

TABLE II Sinter temperature and time for the porous plugs

Plug	Sinter process	Pore structure and porosity	Powder type
A	2 hours/1200°C	Small pores, high porosity	Fine
B	2 hours/1250°C	Small pores, low porosity	Fine
C	2 hours/1250°C	Medium size pores, high porosity	Average
D	4 hours/1575°C and 4 hours/1435°C	Medium size pores, low porosity	Average
E	4 hours/1590°C and 4 hours/1435°C	Large pores, average porosity	Large

3. Physical characterisation of the porous plugs

The physical properties of the plugs were investigated with Mercury Intrusion Porosimetry and SEM. With Mercury Intrusion Porosimetry it is possible to obtain the pore size distribution, pore size and porosity. Mercury Intrusion Porosimetry is a non-destructive test i.e., the test does not destroy the structure and porosity of the samples tested. A typical results obtained with Mercury Intrusion Porosimetry for plug A is shown in Fig. 2.

Fig. 2 shows that there is a narrow pore size distribution with main pore size of about 0.25 μm in size. Fig. 2 also shows that there is no mesoporosity (pores smaller than 10 nm). Due to the application of high sinter temperatures, all these small pores will be closed during the sinter process. Other related parameters that can be extracted form the Mercury Intrusion Porosimetry are the porosity, pore volume and specific surface area. Results are summarized in Table III.

TABLE III Characteristics of the porous plugs

Plug	Description	Porosity (%)	Pore size (μm)	Pore volume (mm^3/g)	Specific surface area (m^2/g)
A	Fine, many pores	24.51	0.25	79.4	4.6
B	Fine, few pores	15.95	0.19	41.9	1.71
C	Average, many pores	22.42	0.7	76	0.8
D	Average, few pores	15.61	1.5	39.5	1.27
E	Large pores	20.25	3	62.1	3.63

All the porous plugs had only one pore size for all the pores, which suggested that the porous plugs had a homogeneous structure. SEM was used to see if the porous material of the plug had indeed a homogeneous structure. The porous plugs were covered by a thin carbon layer, necessary to be able to perform the SEM pictures. A FEG -SEM (Field Emission Gun, Scanning Electron Microscope) was used to obtain the photographs. The results for plug A are shown in Fig. 3.

Fig. 3 showed that the porous plug had a homogeneous structure.

4. Determination of the working characteristics of the porous plug

The working characteristics of interest for the porous plug are: the solution resistance through the plug and the flow through rate of the solution. The flow through rate was measured with an experimental set-up shown in Fig. 4.

The porous plug was fixed in a heat shrinkable Teflon tube. This tube was connected to a pipette. The end of the Teflon tube with the porous plug was soaked in a glass beaker filled with the same solution as the Teflon tube. The pipette was filled with electrolyte solution till a fixed height of approximately 30 cm. Every day the fluid level in the graduated pipette was measured. The

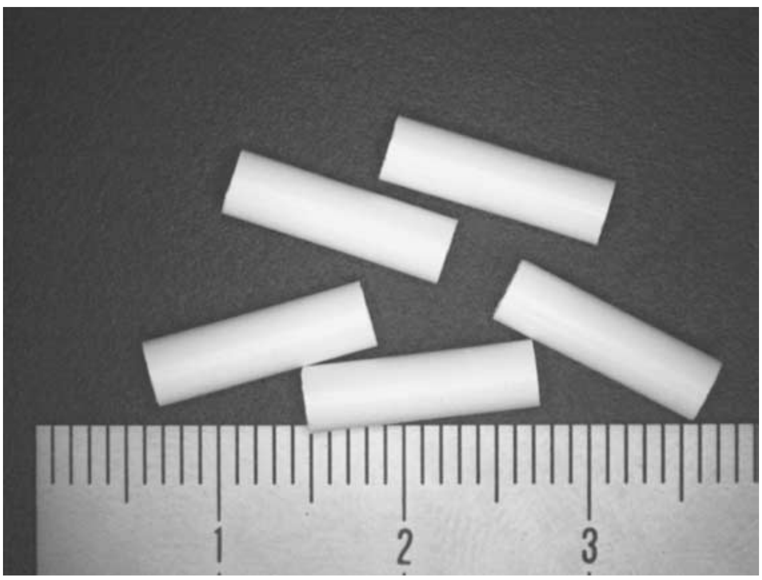

Figure 1 Photograph of the porous zirconia plugs.

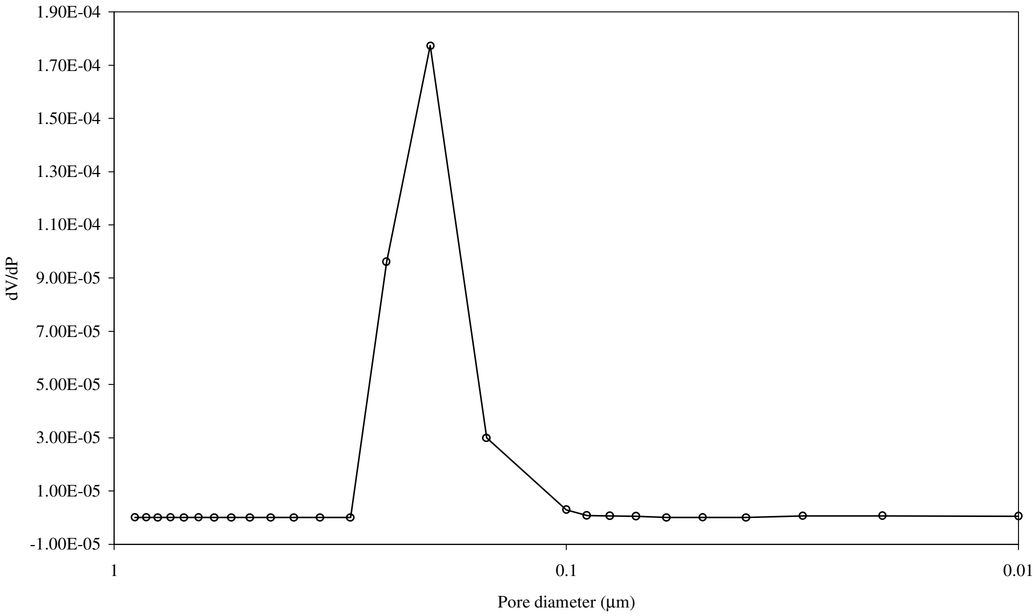

Figure 2 Pore size distribution of porous plug A (small pores, high porosity).

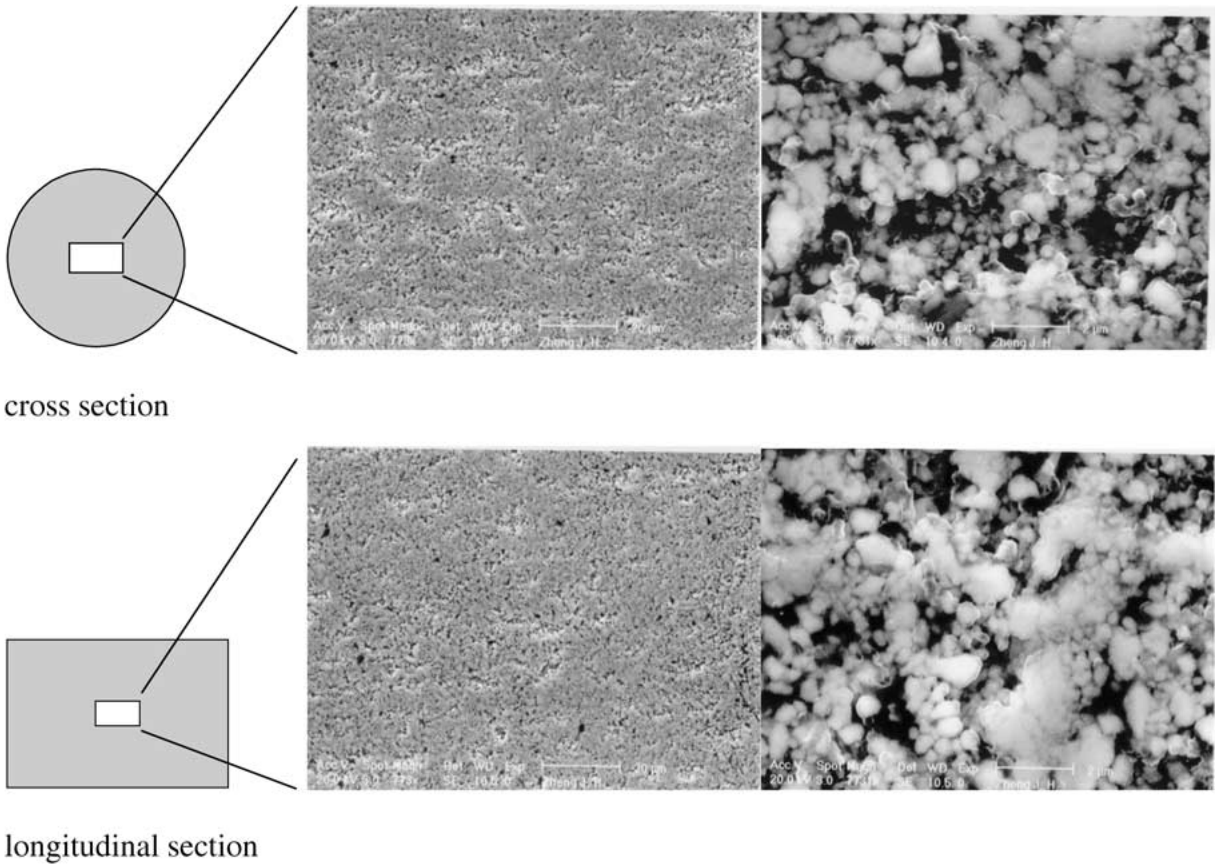

Figure 3 SEM pictures of porous plug A.

measurements would take several weeks. Then the average flow through rate was calculated. A typical value for the fine plugs was 0.2–0.3 μl/hour, which is already better than literature data (1–4 μl/hour) [3].

The influence of a pressure difference along porous plug A was investigated. A silicon tube of 5 meters height was connected to the Teflon tube. This resulted in a pressure increase of 0.5 bar. The flow through rate increased from 0.28 μL/hour to $\pm$115 μL/hour. This showed that care must be taken with pressure variation regarding the use of such ceramic membranes.

The resistance through the plug was determined by a 4 wires ac-measurement [10, 11]. The plugs were soaked in four different solutions, all with a different conductivity. The experimental set-up is shown in Fig. 5.

Four similar stainless steel rods were placed in a glass beaker. All rods were immersed in the solution

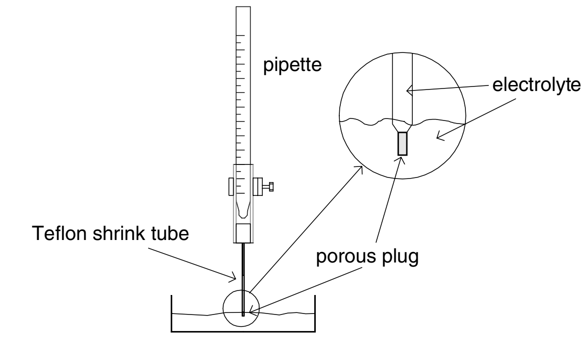

Figure 4 Experimental set-up for flow through rate measurements of porous plugs.

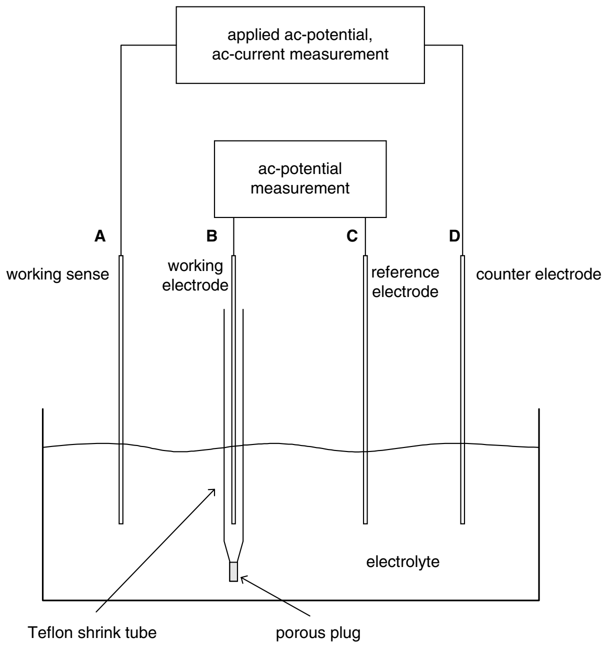

Figure 5 Schematic of the 4-wires ac-measurement; the letters A–D correspond with Fig. 6.

2 cm deep. One of the stainless steel rods was placed in a heat shrinkable Teflon tube containing at one end the porous plug to be investigated. The ac resistance was measured with a Gamry pc3 potentiostat/galvanostat [12]. This device could perform ac-impedance measurements from 100 kHz to less then 1 mHz. Impedance measurements were performed in a frequency range 10 kHz to 10 Hz. At the phase minimum (i.e., phase of the impedance close to zero) the solution resistance could be determined. The electrical equivalent circuit of the experimental set-up is shown in Fig. 6.

At the frequency where the phase of the impedance is zero, both the cable capacitance as the double layer capacity are not contributing to the total impedance and the resistance R_{ohm} is obtained. The measurement is repeated without the porous plug to obtain the resistance of the solution it self. Then the resistance of the solution in the porous plug can be obtained. Results are shown in Table IV.

The data showed that small pores result in a low flow through rate but not necessarily in a high resistance. The resistance did not show a direct relation with the flow through rate.

TABLE IV Flow through rates and resistance measurements of the porous plugs

		Resistance (Ohm/mm)			
Plug	Flow rate (μl/hour)	0.1 M Na_2SO_4	0.1 M KCl	0.01 M KCl	0.001 M KCl
A	0.28	2631	4182	6965	10248
B	0.20	3808	6419	12010	16297
C	23.5	362	497	3121	7036
D	24.2	1909	2463	13455	100918
E	25	1164	6074	15547	47197

5. Mathematical calculation of the porous plug characteristics

To obtain a simple model of the porous plugs, we assume that the pores can be described by a cylindrical tube with radius R and length L. This length is not necessary equal to the length of the porous plug. Then the Hagen-Poiseuille law is assumed to describe the water motion in one cylindrical shaped pore [13, 14]

$$\phi = \frac{\pi R^4}{8\eta}\left(\frac{-\Delta P}{L}\right) \tag{1}$$

where ϕ is the water flux (m^3/s), R is the pore radius (m), η is the dynamic viscosity of water ($\text{Pa} \cdot \text{s}$), ΔP is the pressure difference along a pore (Pa) and L is the pore length (m). Now we assume that a porous plug consists of n parallel positioned pores or tubes. The total flux through the pores is then,

$$\phi = n\frac{\pi R^4}{8\eta}\left(\frac{-\Delta P}{L}\right) \tag{2}$$

where n is the total number of pores in the porous plug.

To obtain an expression for the porous plug impedance, we again assume that we have n parallel pores. The impedance of one pore is then given by,

$$R_{\text{pore}} = \frac{1}{\kappa}\frac{L}{\pi R^2} \tag{3}$$

where κ is the conductivity of the solution (Scm^{-1}). For n pores of similar size and length the total resistance is,

$$\frac{1}{R_{\text{tot}}} = \sum_{i=1}^{n}\frac{1}{R_{\text{pore}}} = \frac{n}{R_{\text{pore}}} = \frac{n\kappa\pi R^2}{L}, \tag{4}$$

$$R_{\text{tot}} = \frac{L}{n\kappa\pi R^2} \tag{5}$$

To determine R_{tot} we need to know the average pore length L, the total number of pores n and the pore radius r. The number of pores n can be expressed as,

$$n = \frac{V_{\text{tot}}}{V_{\text{pore}}} = \frac{\varepsilon V}{\pi R^2 L} \tag{6}$$

where V_{tot} is the total pore volume, V_{pore} is the single pore volume, ε is the porosity and V is the volume of the porous plug.

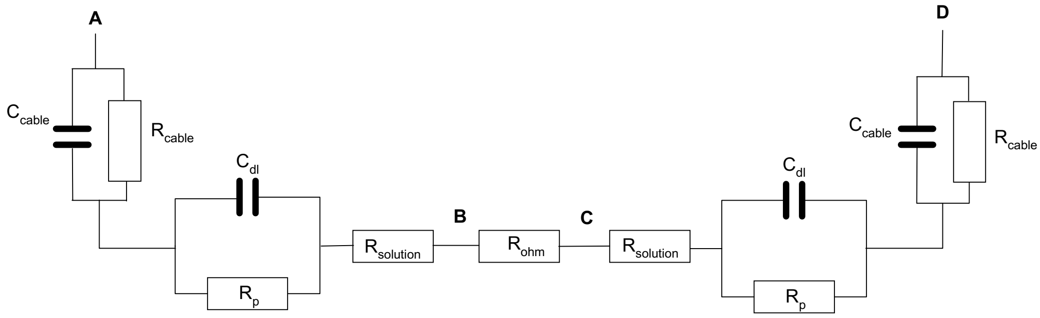

Figure 6 Equivalent circuit representing the frequency dependence of the resistance measurement through the porous plugs; R_{cable} is the cable resistance, C_{cable} is the cable capacitance, R_p is the polarisation resistance of the stainless steel electrodes, C_{dl} is the double layer capacity of the electrodes, $R_{solution}$ the solution resistance and R_{ohm} is the electrolyte resistance between the electrodes B and C including the porous plug. The letters A–D correspond with Fig. 5.

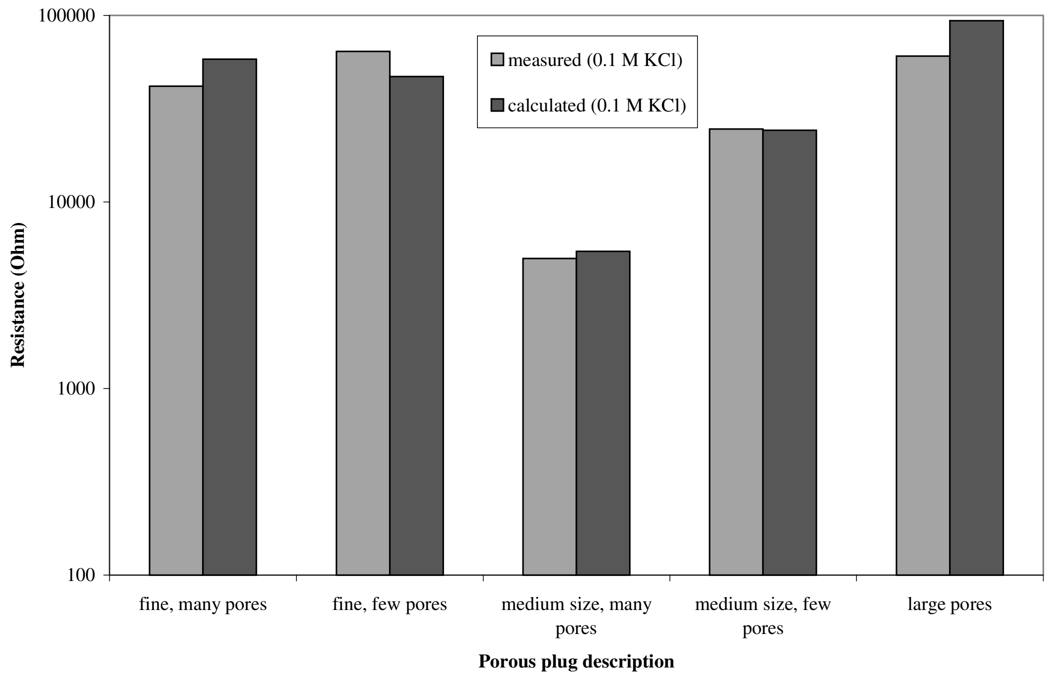

Figure 7 Measured and calculated resistance of porous plugs filled with 0.1 M KCl.

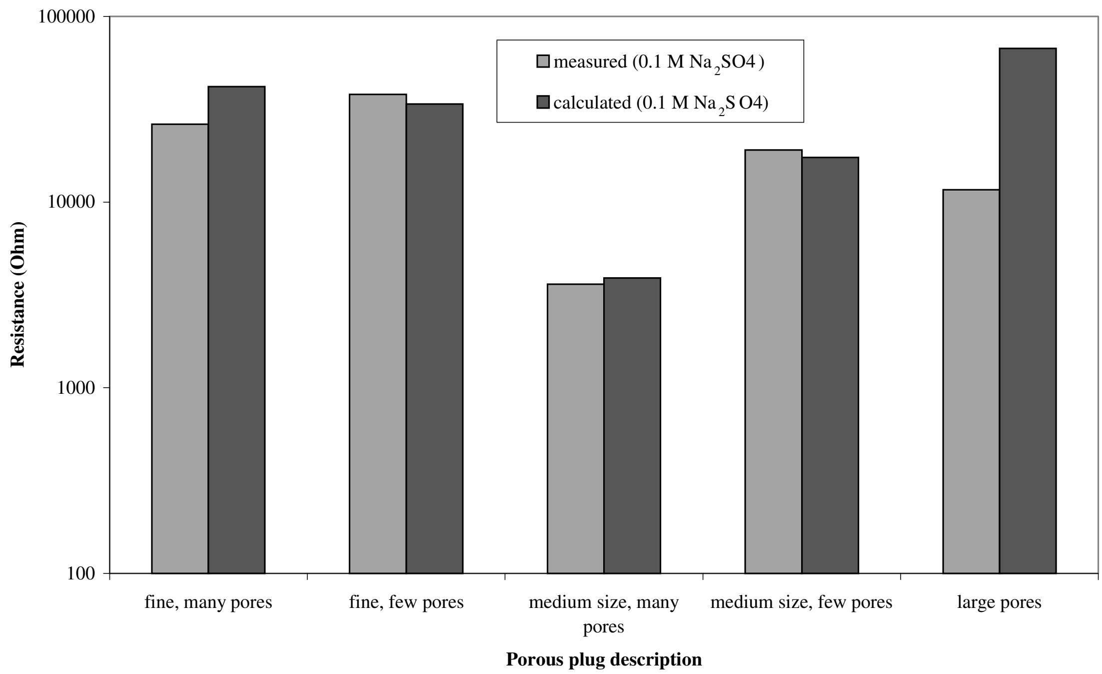

Figure 8 Measured and calculated resistance of porous plugs filled with 0.1 M Na_2SO_4.

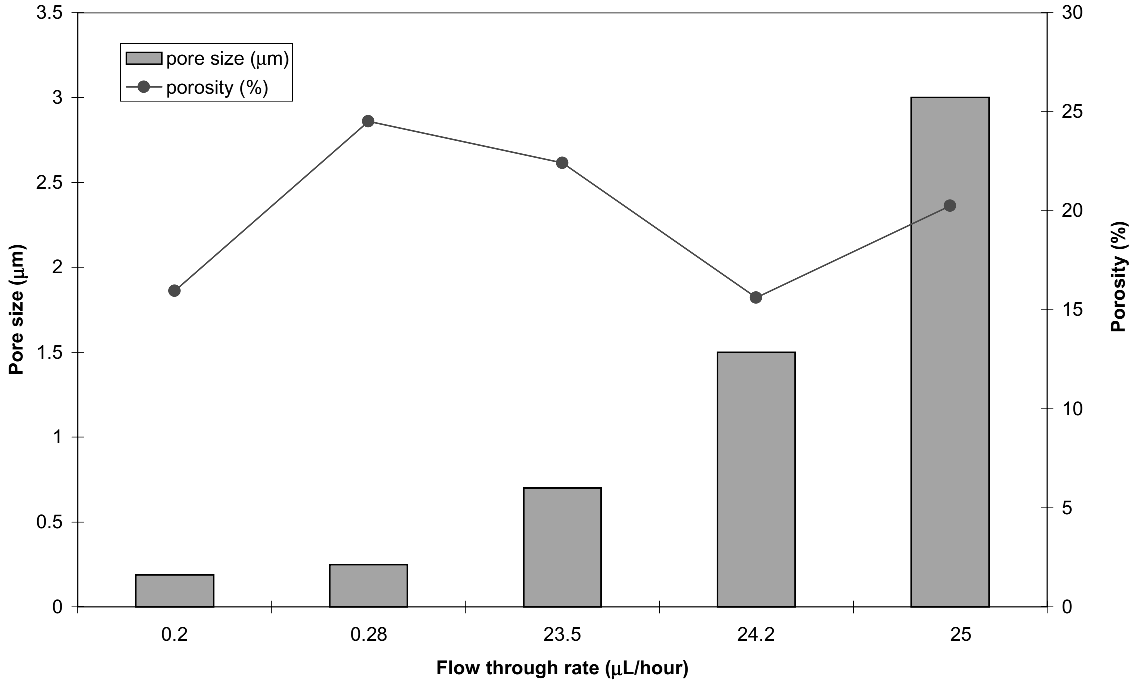

Figure 9 Relation between pore size, porosity and flow through rate.

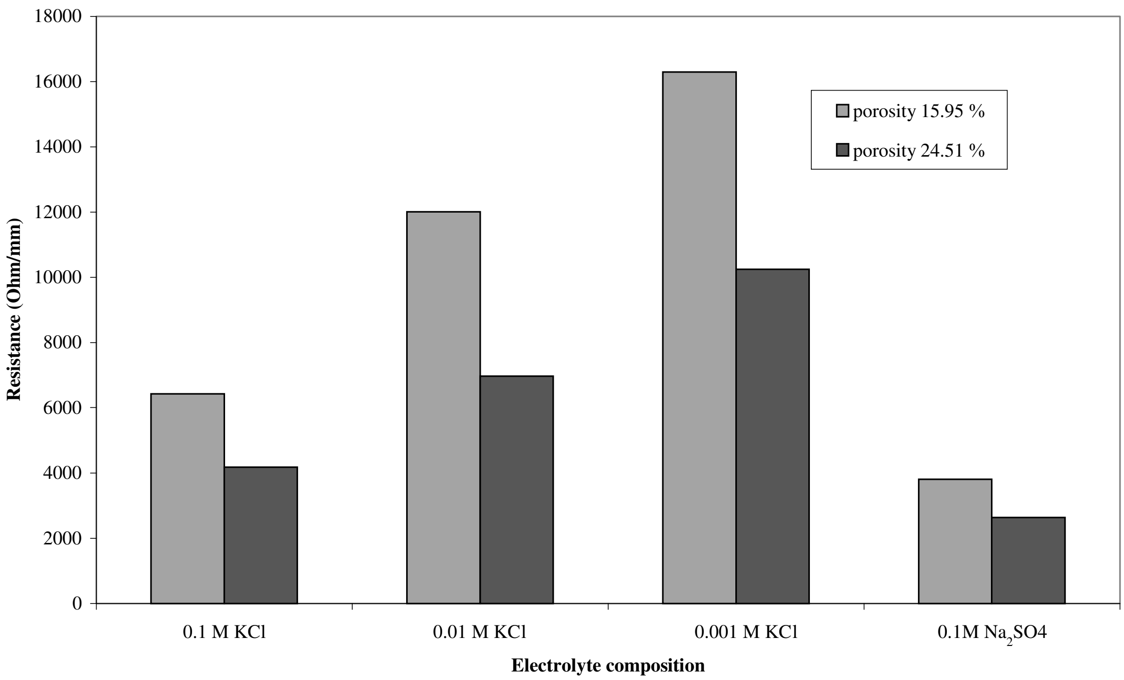

Figure 10 Relation between the porosity and the resistance through the plug for the fine plugs A and B for solutions with different conductivity's.

Equation 6 can be substituted in Equation 2 resulting in,

$$\phi = \frac{\pi R^2}{8\eta}\left(\frac{-\Delta P}{L^2}\right)\varepsilon V \tag{7}$$

solving for L,

$$L = \sqrt{\frac{\pi R^2}{8\eta}\left(\frac{-\Delta P}{\phi}\right)\varepsilon V} \tag{8}$$

It is now possible to calculate the total (ionic) resistance of a porous plug filled with electrolyte solution. The known parameters are the dynamic viscosity of water η, the water flux ϕ, the porosity ε, the specific conductivity κ, the pore radius R (from Mercury Intrusion Porosimetry), the volume of the porous plug V and the pressure drop along the pore ΔP. First the average pore length L is calculated with Equation 8. Then the total number of pores is calculated with Equation 6. Finally the total resistance R_{tot} can be determined with Equation 5.

6. Results and discussion

Fig. 7 shows a comparison between the measured and calculated values for the resistance (R_{tot}) of a porous plug soaked with a solution of 0.1 M KCl

($\kappa = 0.01289$ Scm^{-1} [15]) and Fig. 8 shows a comparison between the measured and calculated values of R_{tot} for 0.1 M Na_2SO_4 ($\kappa = 0.01799$ Scm^{-1} [15]). It can be seen that there is good agreement between the mathematical and experimental results.

The relation between the flow through rate and pore size and porosity is shown in Fig. 9.

Fig. 9 shows that the flow through rate mainly depends on the pore size. This seems logic regarding the capillary action of small pores. Fig. 10 shows the relation between the porosity and the resistance through the porous plugs for four different solutions for plug A and B (plugs with similar pore size).

For similar pore sizes (i.e., plugs A and B) the porosity determined the resistance through the plug as can be seen from Fig. 10. If there is more space for liquid (electrolyte) in the plug, there are more opportunities for conductance and the resistance decreases. The results were quite reproducible as for all four electrolyte solutions, similar results were obtained.

Based on these results the optimum design for a porous plug was a plug with high porosity and small pores. In this case plug A had the smallest pores in combination with the highest porosity and was the plug with the best performance.

7. Conclusions

Four different measurement techniques were employed to characterise a porous ceramic plug to be used in electrochemical sensors. These techniques were Mercury Intrusion Porosimetrie and SEM to obtain the physical characteristics of the porous plug and ac-resistance measurements and flow through rate measurements to obtain the working characteristics of the porous plug. It was shown that with these techniques it was possible to find the optimised design of a porous plug. The porous plug with the best performance was plug A having small pores (± 0.25 μm) and a relative large porosity ($\pm 25\%$). Also a simple mathematical model based on the Hagen-Poiseuille equation was developed to describe the porous plug characteristics. It was shown that mathematical and experimental values of the porous plug resistance were in good agreement.

References

1. D. J. G. IVES and G. J. JANZ, in "Reference Electrodes, Theory and Practice" (Academic Press, New York, London, 1961, reprinted by NACE 1996).
2. D. PLETCHER and F. C. WALSH, in "Industrial Electrochemistry" (Blackie Academic & Professional, London, 1993) p. 603.
3. U. TINNER, in "Electrodes in Potentiometry" (Monograph, Metrohm Ion Analysis, Switzerland).
4. M. E. INDIG, *Corrosion* **46** (1990) 680.
5. M. J. DANIELSON, *ibid.* **39** (1983) 202.
6. *Idem.*, *ibid.* **35** (1979) 200.
7. D. D. MACDONALD, *ibid.* **34** (1978) 75.
8. D. D. MACDONALD, A. C. SCOTT and P. WENTRCEK, *J. Electrochem. Soc.* **126** (1979) 1618.
9. *Idem.*, *ibid.* **126** (1979) 908.
10. J. R. MACDONALD, in "Impedance Spectroscopy, Emphasizing Solid Materials and Systems" (John Wiley & Sons, New York, 1987).
11. R. COTTIS and S. TURGOOSE, in "Electrochemical Impedance and Noise, Corrosion Testing Made Easy" (NACE International, 1999).
12. Gamry PC-3/300 Potentiostat/Galvanostat, EIS300 Electrochemical Impedance Spectroscopy System, 1996.
13. A. LEVENTIS, D. A. VERGANELAKIS, M. R. HALSE, J. B. WEBBER and J. H. STRANGE, *Transport in Porous Media* **39** (2000) 143.
14. J. M. SMITHS, E. STAMMERS and L. P. B. M. JANSSEN, "Fysische Transportverschijnselen" (Delftse Uitgevers Maatschappij, Delft, 1989) p. 28.
15. CRC Handbook of Chemistry and Physics, 79th edn. (CRC Press 1998/1999) p. 5.

Received 18 April 2001
and accepted 14 May 2002